

Crystal structure of human calmodulin-like protein: insights into its functional role¹

Bong-Gyoon Han, Minhua Han², Haixin Sui, Paul Yaswen, Peter J. Walian, Bing K. Jap*

Life Sciences Division, Lawrence Berkeley National Laboratory, University of California, Berkeley, CA 94720, USA

Received 14 March 2002; accepted 23 April 2002

First published online 23 May 2002

Edited by Takashi Gojobori

Abstract A calmodulin (CaM)-like protein (hCLP) is expressed in human mammary epithelial cells but appears to be limited to certain epithelial cells such as those found in skin, prostate, breast and cervical tissues. A decrease in the expression of this protein is associated with the occurrence of tumors in breast epithelium. The structure of hCLP determined to 1.5 Å resolution by X-ray crystallography shows a distinct 30° displacement along the interconnecting central helix, when compared to the highly conserved structure of vertebrate CaM, resulting in a difference in the relative orientation of its two globular domains. Additionally, the electric surface potential landscape at the target protein binding regions on the two globular domains of hCLP is significantly different from those of CaM, indicating that the respective ranges of hCLP and hCaM target proteins do not fully overlap. Observations that hCLP can competitively inhibit CaM activation of target proteins also imply a role for hCLP in which it may also serve as a modulator of CaM activity in the epithelial cells where hCLP is expressed. © 2002 Published by Elsevier Science B.V. on behalf of the Federation of European Biochemical Societies.

Key words: Crystal structure; Calmodulin; hCLP

1. Introduction

Calmodulin (CaM) is a highly conserved Ca²⁺ binding protein, which is ubiquitous and central in translating Ca²⁺ levels into physiological signals. The crystal structures of Ca²⁺ bound CaM show that this protein contains two similar domain structures linked by an extended α -helix [1–6], each domain containing two helix-loop-helix EF-hand Ca²⁺ binding motifs. The incorporation of Ca²⁺ into CaM is essential and leads to a major conformational change which includes the opening of a hydrophobic cavity in each globular domain necessary for target protein recognition [7]. Various modes of target peptide recognition have been reported [8–15] and the hydrophobic patches of the globular domains together with the charged residues around their rims are believed to be key for target recognition and specificity.

A human CaM-like protein (hCLP) has been identified [16]

and found to have 85% sequence identity compared to human CaM (hCaM). It has a higher content of basic residues (11 Arg and seven Lys) compared to hCaM (six Arg and eight Lys), resulting in an overall more basic protein [17]. Co-immunoprecipitation data indicate that the main hCLP binding protein in vivo is an unconventional myosin I species of approximately 116 kDa, suggesting that hCLP functions as a myosin binding partner in vivo (Yaswen and Hosoda, unpublished data). Despite the high sequence identity of hCLP and hCaM, their expressions and biochemical properties are quite distinct. While the expression of CaM is ubiquitous, the expression of hCLP is localized to special types of epithelial cells such as breast, prostate, skin and cervix. In addition, the expression of this protein in human mammary epithelial cells decreases drastically in corresponding tumor tissues [18,19]. Activation of target proteins by hCLP is different from that of CaM. For example, the activation of CaM-dependent enzymes (cAMP phosphodiesterase, calcineurin, nitric oxide synthase, and myosin-light chain kinase) by hCLP is much weaker and, in the case of myosin-light chain kinase as a target protein, it competitively inhibits CaM activation [20].

hCLP is not able to substitute for yeast CaM (yCaM) [21]. Although the amino acid sequences of yCaM and hCLP show that there are 64 amino acids different, only three non-conserved residues (Arg-57, Arg-111, Ala-127) have been found to affect hCLP's ability to substitute for yCaM. In CaM, these residues are located along the rims of its target protein binding regions. In this paper, we report the 1.5 Å crystal structure of the hCLP protein that reveals features distinct from those of CaM: the surface potential landscapes of the globular domains and central helix flexibility of hCLP and CaM are notably different. These differences are discussed in context to their interactions with target proteins and their functional roles.

2. Materials and methods

2.1. Crystallization

hCLP cDNA was amplified by polymerase chain reaction from total normal human mammary epithelial cell cDNA and cloned into a plasmid pET-NB-1 [18]. hCLP was expressed in *Escherichia coli* and purified using phenyl Sepharose CL-4B hydrophobic and DEAE ion exchange chromatography. Crystals were obtained by the sitting-drop technique utilizing a vapor diffusion procedure. In the crystallization wells, the protein, which was concentrated to 7 mg/ml in 50 mM pH 7.5 Tris buffer containing 2 mM CaCl₂, was mixed with mother liquor containing 27% MPD, 15% ethanol, 50 mM CaCl₂ and 0.1 M sodium acetate buffer pH 4.5 in a 3:1 volume ratio. Crystals were normally harvested in 1–2 weeks. Crystals belong to the space group P2₁2₁2 with unit cell dimensions, $a=63.3$, $b=93.5$, $c=24.8$ Å, $\alpha=\beta=\gamma=90^\circ$.

*Corresponding author.

E-mail address: bkjap@lbl.gov (B.K. Jap).

¹ The atomic coordinates have been deposited with the RCSB Protein Data Bank (PDB), under entry code 1GGZ.

² Present address: Chiron Corporation, Emeryville, CA 94608, USA.

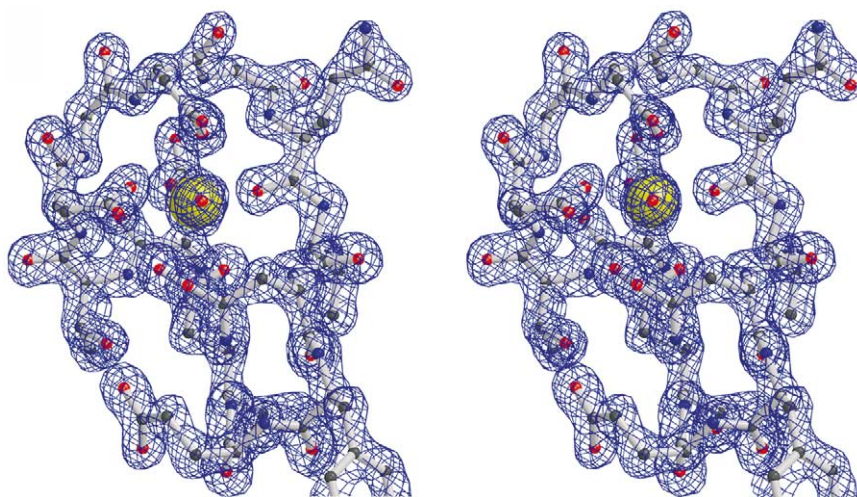


Fig. 1. Stereoview of the $2|F_o| - |F_c|$ electron density map in one of the Ca^{2+} binding regions (residues 129–140) contoured at 1.5σ . Ca^{2+} ion is represented as a yellow ball.

A selenomethionine (SeMet)-substituted form of hCLP protein [22] was crystallized under conditions similar to those of the native protein.

2.2. Data collection, phasing, model building, and refinement

The molecular structure was determined to about 1.5 Å resolution by multiple wavelength anomalous dispersion (MAD) techniques using SeMet-labeled protein (Table 1). Diffraction data were collected at the Advanced Light Source (ALS) of the Lawrence Berkeley National Laboratory under cryo-conditions with mother liquor as cryo-protectant and processed with DENZO/SCALEPACK [23]. The eight selenium sites per asymmetric unit were located with the program SOLVE [24].

Subsequent phase modification including solvent flattening was accomplished using DM [25] to 1.5 Å resolution, producing an easily interpretable map (Fig. 1). Model building was performed using O [26]. Energy minimization and simulated annealing-based refinement of the model was performed using the 'Crystallographic and nuclear magnetic resonance (NMR) system' [27]. In the last round of refinement, water was added. A final R value of 18.3 and an R_{free} value of 22.1 were obtained.

3. Results and discussion

3.1. Comparison of hCLP and CaM general architectures

The general structural motif of the hCLP is very similar to CaM, consisting of a dumbbell-like structure containing two globular domains connected by a central seven-turn, α -helix (Fig. 2a,b). The structure contains a total of seven α -helices; residues 5–20 (helix A), 28–39 (helix B), 44–54 (helix C), 65–92 (helix D), 101–112 (helix E), 117–129 (helix F), and 138–147 (helix G), comprising about 69% of the total amino acid residues. The hCLP central α -helix (helix D) is the most hydrophilic; it also has the highest temperature factors that are, however, significantly lower than the equivalent values for hCaM. The N- and C-terminal globular domains consist of three α -helices each and contain hydrophobic residues accessible to solvent (Fig. 2a,b); their α -carbon backbones are nearly superimposable. Each globular domain contains two

Table 1
Data collection and structure refinement statistics

Set	Space group	Wavelength (Å)	Resolution (Å)	Redundancy	I/σ_I	Completeness (%)	R_{sym} (%)
MAD							
edge	P2 ₁ 2 ₁ 2	0.9798	30–1.8 (1.83–1.8)	4.93 (4.91)	18.9 (17.9)	97.5 (97.4)	6.1 (9.7)
peak	P2 ₁ 2 ₁ 2	0.9795	30–1.8 (1.83–1.8)	7.19 (7.15)	25.8 (19.9)	100.0 (100.0)	7.2 (14.5)
distant	P2 ₁ 2 ₁ 2	0.9649	30–1.8 (1.83–1.8)	6.83 (6.8)	23.7 (13.2)	99.9 (100.0)	6.3 (17.2)
Native	P2 ₁ 2 ₁ 2	1.000	20–1.5 (1.53–1.5)	5.57 (2.58)	30.5 (5.0)	97.7 (78.7)	4.3 (20.8)
Reflections in working set				22 600			
Reflections in test set				1 153			
R_{free} (%)				22.1			
R (%)				18.3			
R.m.s. bond lengths (Å)				0.0097			
R.m.s. bond angles (°)				1.64			
Number of non-hydrogen atoms				1 142			
Number of solvent atoms				200			
Ramachandran plot (%)							
residues in most favored regions				96.1			
residues in additional allowed regions				3.9			
Average B factor (Å ²)							
main chain				14			
side chain				20			

$R_{\text{sym}} = \sum |I - \langle I \rangle| / \sum I$, where I is the measurement of intensity. $R = \sum |F_{\text{obs}} - F_{\text{calc}}| / \sum F_{\text{obs}}$ for all values where F_{obs} is the observed native amplitude and F_{calc} is the one calculated from atomic models. R_{free} is the R value for 5% of the total reflections that were excluded in refinement. The values for the highest resolution zone are shown in parentheses.

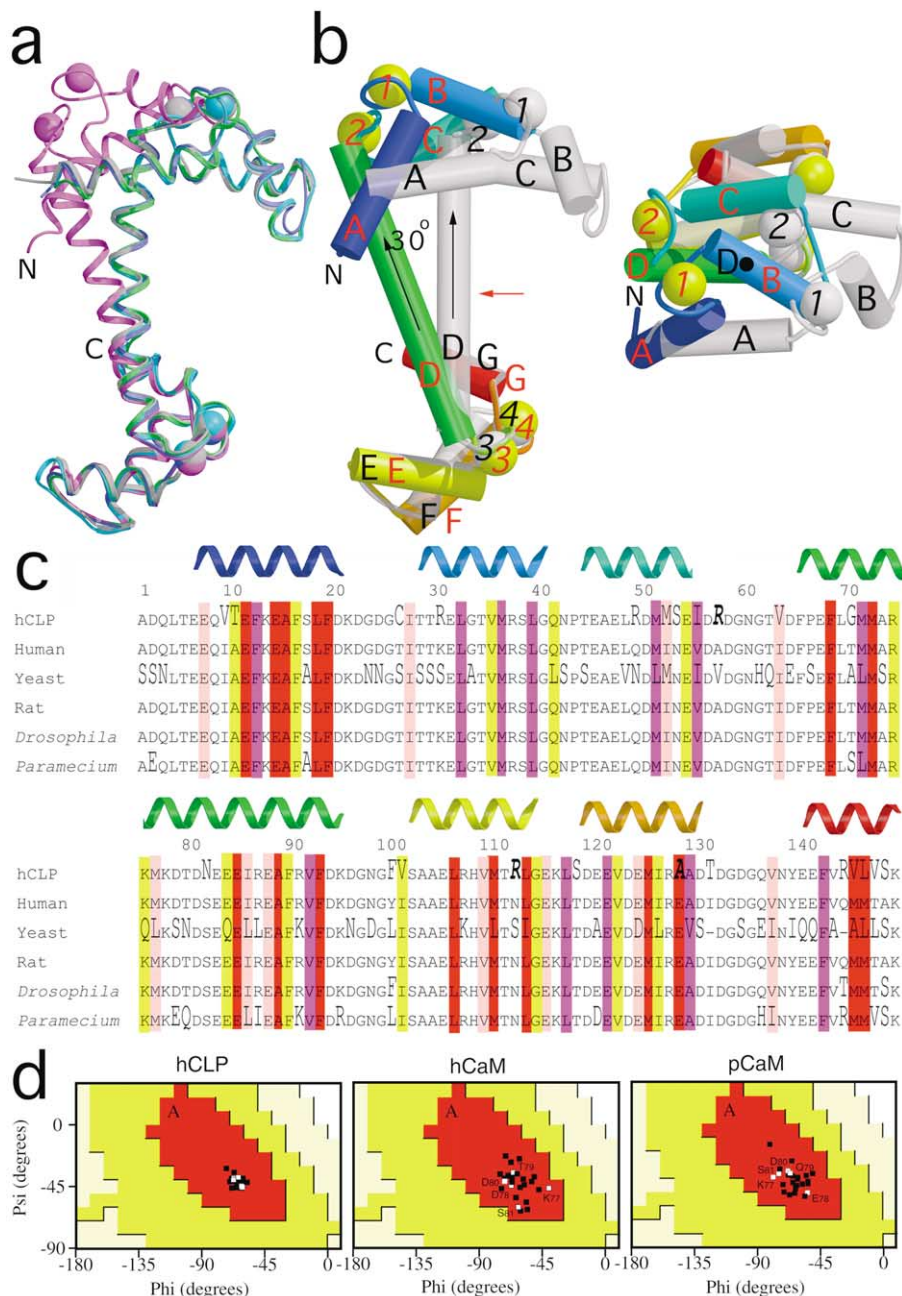


Fig. 2. Schematic diagrams, sequence comparison, and Ramachandran plots. a: Superposition of hCLP and four CaMs in ribbon diagram format. Each molecule is shown in a different color (hCLP, purple; hCaM, light blue; rCaM, cyan; *Drosophila* CaM (dCaM), light green; *Paramecium* CaM (pCaM), gray). b: Side and top view of a superposition of hCLP and hCaM. α -Helices are shown as cylinders and labeled (hCaM is labeled black and hCLP red) alphabetically from the N- to C-terminus. Ca^{2+} ions are shown as balls and labeled numerically beginning at the N-terminus. hCaM is shown in translucent white while hCLP polypeptides are colored blue to red from the N- to C-terminus and hCLP Ca^{2+} ions are colored yellow. The two molecules are brought into register using the α -carbons from C-terminal amino acid residues 93–147. For the side view, the two molecules are oriented so that the central helix D of hCaM is positioned parallel to the plane of the paper. The D helices of hCaM and hCLP are displaced by 30° . For the top view, the two molecules are rotated around the axis shown as the red arrow. Helix D of hCaM is hidden from the view and the helix axis is denoted by a black circle. For the top view, only the N-terminal domains and central helix D are labeled. c: The sequence comparison of hCLP and CaMs from human, yeast, rat, *Drosophila*, and *Paramecium*. Large letters indicate amino acid residues which are different from hCaM. Three residues, which were studied by point mutation in hCLP, are written in large bold letters. Amino acid residues which make contact with target peptides in hCaM from four published CaM and peptide [8–11] are shown in colored boxes. The amino acid residues which make contact with target peptides in all four published complex structures are colored red, three purple, two pink, and one yellow. d: Ramachandran plot of the central helix (residues 65–92) for hCLP, hCaM and pCaM. The five residues in the central part of the helix (amino acid residues 77–81), which has been shown to be the most flexible region in CaM by NMR studies, are denoted by white squares and are labeled in the case of hCaM and pCaM. The figures (a) and (b) were produced using the program MOLSCRIPT [28] and Raster3D [29].

EF-hand (helix-loop-helix) motifs which form the four Ca^{2+} binding sites.

While at the α -carbon backbone level the globular domains of hCLP and various CaMs are very similar, significant differences can be found in their central helix regions (Table 2). The root mean square (r.m.s.) deviation between hCLP and the CaMs is greatest along the central helix despite the fact that this is also the region of highest sequence homology. When the C-terminal globular domains of hCLP and hCaM are superimposed, there is a 30° offset of the N-terminal globular domains between the two molecules as shown in Fig. 2b. This offset is brought about by the difference in the curvatures of the central helices and a difference in the orientation of the globular domains about the hinge regions.

3.2. Central helix

As mentioned above, the central helix (Phe-65–Phe-92) of hCLP is substantially different from that of CaM and shows a significant relative displacement (Fig. 1a). The mobile nature of the central helix of CaM has been well documented. NMR studies of CaM have shown that the middle region of the central helix (Lys-77–Ser-81) is quite flexible [30]; the crystallographic hCaM data show that residues Thr-79–Ser-81 of hCaM adopt a non-ideal α -helical conformation and have the highest temperature factors ($B=44 \text{ \AA}^2$) [4], supporting dynamic conformational changes that allow for the two globular domains to interact with target proteins. In contrast, temperature factors of the corresponding residues in hCLP are significantly lower ($B=19 \text{ \AA}^2$). The lower temperature factor of this region in hCLP is not likely to be the result of crystal packing since it is not involved in the formation of crystal contacts. Furthermore, the central helix (residues 65–92) of hCLP has a more uniform helical structure than the corresponding regions of hCaM with psi and phi angles close to the ideal values of -39.4° and -65.3° respectively

(Fig. 2d). The distribution of psi and phi angles in this region of the pCaM model structure even at near atomic resolution (1.0 \AA) is significantly broader than those from the corresponding region of the hCLP model structure, further suggesting that the central helix of hCLP is less flexible compared to CaM.

The flexible and unwinding nature of the central helix middle region is clearly critical for the ability of CaM to wrap around proteins and accommodate various kinds of targets. A reduction in this flexibility would therefore alter the ability of the globular domains to move relative to each other and attain the conformation necessary for binding to target peptides. This difference in flexibility may result in a significant difference in the types of hCLP and CaM target protein interactions possible. Interestingly, the recent structure of CaM complexed with anthrax edema factor reveals a relatively extended form of CaM bound to its target indicating that a ‘wrapping’ mechanism is not the only mode of binding leading to target activation [14].

3.3. Globular domains

Within the target protein binding regions of the globular domains, hCLP contains several residues that are different from those found in CaM (Figs. 3 and 4). hCaM residue Glu-127, located on the rim of the target protein binding region of the C-terminal globular domain, has been found to make a salt bridge with an Arg residue on its target peptide. The replacement of Glu-127 with Ala, as found in hCLP, affects not only Ca^{2+} binding affinity but also changes the electric potential landscape of one of its target protein binding regions clearly influencing the nature of target proteins it can successfully interact with. In fact, it has been shown that phosphorylation of Ser-458 of CaM target protein Ca^{2+} /CaM-dependent protein kinase kinase (CaMKK) abolishes CaMKK activity [31,32]; Ser-458 is located in close proximity

Table 2
R.m.s. (\AA) fit comparison of various hCLP and CaM backbone regions

Protein (PDB ID)	Source	Resolution (\AA)	Residue number	R.m.s. fit (\AA)	Sequence identity (%)
hCaM (1CLL)	human	1.7			
N-domain			4–64	0.0	100
Central helix			65–92	0.0	100
C-domain			93–147	0.0	100
Total			4–147	0.0	100
rCaM (3CLN)	rat	2.2			
N-domain			5–64	0.19	100
Central helix			65–92	0.30	100
C-domain			93–147	0.23	100
Total			5–147	0.28	100
dCaM (4CLN)	<i>Drosophila</i>	2.2			
N-domain			4–64	0.89	100
Central helix			65–92	0.38	100
C-domain			93–147	0.62	94.5
Total			4–147	0.77	98.0
pCaM (1EXR)	<i>Paramecium</i>	1.0			
N-domain			4–64	0.99	98.4
Central helix			65–92	0.92	75.0
C-domain			93–147	0.73	85.5
Total			4–147	1.05	88.4
hCLP (1GGZ)	human	1.5			
N-domain			4–64	1.12	83.6
Central helix			65–92	1.33	92.9
C-domain			93–147	0.61	80.0
Total			4–147	3.84	84.4

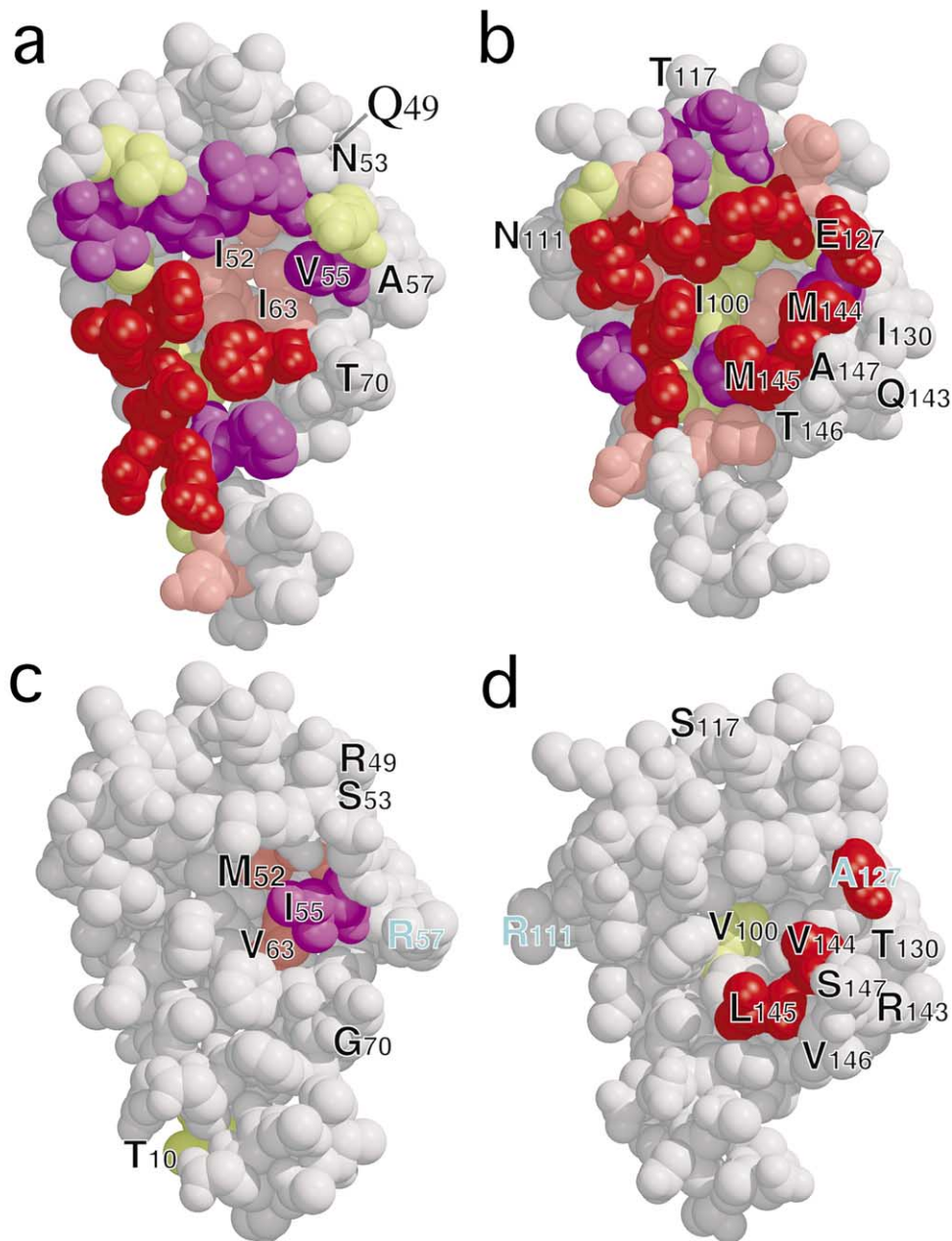


Fig. 3. Space filling representation of hCaM and hCLP with the emphasis on target peptide binding sites. Amino acid residues, which are different in hCaM and hCLP, are labeled. Three residues (Arg-57, Arg-111, Ala-127) in hCLP, which have been studied by point mutation in yeast, have cyan-colored labels. For (a) and (b), the same coloring scheme as Fig. 2c has been used for the amino acid residues which make contact with target peptides. In (c) and (d), a similar color scheme has been used for the corresponding amino acid residues but only those residues which are different in both molecules are colored for simplicity. a: N-terminal globular domain (residues 4–70) of hCaM. b: C-terminal globular domain (residues 78–147) of hCaM. c: N-terminal globular domain of hCLP. d: C-terminal globular domain of hCLP.

to Glu-127 and its phosphorylation would destabilize the salt bridge formed between Glu-127 and its binding partners on CaMKK [11]. These results suggest that target proteins that are selective for hCLP would likely contain residues that allow for favorable interactions with Ala-127. In the hCLP structure, residues Arg-57 and Arg-111 are also located at the periphery of the target protein binding regions of the N-terminal and C-terminal globular domains respectively (Figs. 3 and 4). Since charged residues at the vicinity of the binding domains in CaM are known to play an important role in CaM target protein binding, replacement of uncharged residues

(Ala-57 and Asn-111 of hCaM) with positively charged Arg can be expected to affect the target protein binding interactions as well as Ca^{2+} binding affinity. It is therefore not surprising that point mutation studies in yeast show that residues Glu-127, Ala-57 and Asn-111 are important for the activity of CaM [21] in cell growth.

In addition to the above three non-conservatively substituted residues, there are several conservative substitutions. In the C-terminal globular domain of hCaM residues Met-144, Met-145 and Ile-100, which are positioned within the hydrophobic patch of the target binding region, are replaced

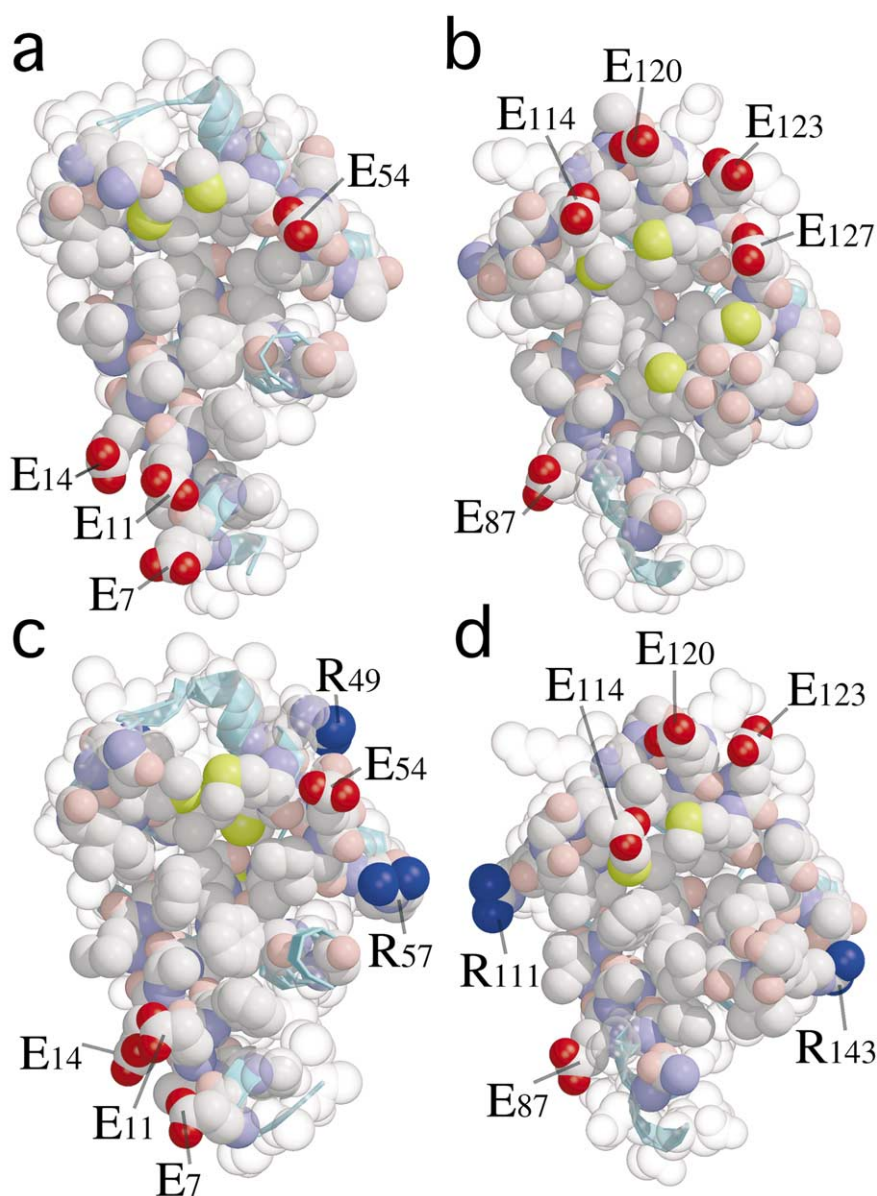


Fig. 4. Space filling representation of hCaM and hCLP in the same orientation as Fig. 3 but with an emphasis on the electric potential landscapes around the peptide binding sites. Residues which are known to be involved in target peptide binding from previous structural studies of CaM and residues which differ in hCLP and hCaM are all shown as solid spheres: other residues are shown as translucent spheres. The carbon atoms are colored white, carboxyl oxygens red, other oxygens pink, nitrogens from arginines blue, other nitrogens light blue, and sulfurs yellow. The figures were prepared in the same orientation as in Fig. 3. Charged residues are labeled. a: N-terminal globular domain (residues 4–70) of hCaM. b: C-terminal globular domain (residues 78–147) of hCaM. c: N-terminal globular domain of hCLP. d: C-terminal globular domain of hCLP. The glutamic acids identified in (a) and (b) are known to frequently interact with residues of the target peptides as discussed in the text. These residues add an additional dimension of flexibility in target selection.

in hCLP by Val, Leu and Val respectively (Fig. 3). In the N-terminal globular domain, residues Ile-52, Val-55 and Ile-63 of hCaM, which again are all positioned within the hydrophobic patch of a target binding region, are replaced respectively with Met, Ile and Val in hCLP (Fig. 3). Similar conservative substitutions are also found in fully functional yCaM and appear to be well tolerated without significant alteration of CaM function.

The differences in globular domain residues, particularly those located within the target protein binding regions of the globular domains, are expected to affect the four Ca^{2+} binding sites. It has been reported that there is a 10-fold

weaker Ca^{2+} binding affinity in hCLP compared to hCaM [17]. Since the α -carbon backbones of globular domains of hCLP and hCaM are highly conserved, the difference in Ca^{2+} binding is likely to be the result of the relatively smaller negative surface charge of the hCLP globular domains. A simple electric potential energy calculation (based on AMBER electrostatic parameters [33]) indicates that the relative binding energies of Ca^{2+} for the N- and C-terminal domains of hCLP are significantly smaller than those for the equivalent domains of hCaM. hCLP's weaker binding affinity for Ca^{2+} suggests that it has a different Ca^{2+} -mediated response as compared to CaM. It appears then that under normal phys-

iological levels of Ca^{2+} , hCLP could compete for binding with CaM target proteins in circumstances where target binding does not require the presence of Ca^{2+} in the binding globular domains. Radically decreased expression levels of hCLP, such as those found in breast tumor tissues [18], together with its unique electric potential landscapes and less flexible central helix, would therefore be expected to affect any CaM modulation role. Along this line, it is interesting to note that a decrease in the expression level of hCLP is associated with early events in breast cancer development [19].

Of the various proteins from which the structures of their complexes with CaM have been determined [8–14], two, CaM kinase II and myosin-light chain kinase, have been studied for their interaction with hCLP [20]. hCLP activates CaM kinase II and competitively inhibits CaM-dependent activation of myosin-light chain kinase while CaM activates both proteins. The differences in target protein interactions are likely the result of the difference in the mobility of central helix that may prevent activation of certain targets by hCLP and/or residue substitutions that alter the electrical potential landscape of the target protein binding domains as well as Ca^{2+} binding affinity.

In summary, the structural differences of hCLP and CaM, especially as reflected in the electric potential landscapes, have provided insight into probable functional properties of hCLP. Altering charged residues along the rim of the target binding domains modifies the range and strength of interaction with target proteins. The presence of more basic residues in the target protein binding domains of hCLP, affecting both Ca^{2+} and target protein binding, and the lower flexibility of the CLP central helix suggest the existence of hCLP specific target proteins and a potential role in CaM activity modulation. The presence of hCLP target proteins in the epithelial cells in which they are specifically expressed has yet to be firmly established, although an unconventional myosin I species has been found to be one possible candidate (Yaswen and Hosoda, unpublished results).

Acknowledgements: This work was supported by the Director, Office of Science, Office of Biological and Environment Research, Life Sciences Division, of the U.S. Department of Energy (DOE) and by National Institutes of Health (NIH) Research Grants (GM58593). We also thank the staff at the ALS beam line 5.0.2 for their assistance during data collection and John K. Lee for software support.

References

- [1] Babu, Y.S., Sack, J.S., Greenhough, T.J., Bugg, C.E., Means, A.R. and Cook, W.J. (1985) *Nature* 315, 37–40.
- [2] Babu, Y.S., Bugg, C.E. and Cook, W.J. (1988) *J. Mol. Biol.* 204, 191–204.
- [3] Taylor, D.A., Sack, J.S., Maune, J.F., Beckingham, K. and Quijoch, F.A. (1991) *J. Biol. Chem.* 266, 21375–21380.
- [4] Chattopadhyaya, R., Meador, W.E., Means, A.R. and Quijoch, F.A. (1992) *J. Mol. Biol.* 228, 1177–1192.
- [5] Rao, S.T., Wu, S., Satyshur, K.A., Ling, K.Y., Kung, C. and Sundaralingam, M. (1993) *Protein Sci.* 2, 436–447.
- [6] Wilson, M.A. and Brünger, A.T. (2000) *J. Mol. Biol.* 301, 1237–1256.
- [7] Zhang, M., Tanaka, T. and Ikura, M. (1995) *Nat. Struct. Biol.* 2, 758–767.
- [8] Ikura, M., Clore, G.M., Gronenborn, A.M., Zhu, G., Klee, C.B. and Bax, A. (1992) *Science* 256, 632–638.
- [9] Meador, W.E., Means, A.R. and Quijoch, F.A. (1992) *Science* 257, 1251–1255.
- [10] Meador, W.E., Means, A.R. and Quijoch, F.A. (1993) *Science* 262, 1718–1721.
- [11] Osawa, M., Tokumitsu, H., Swindells, M.B., Kurihara, H., Orita, M., Shibamura, T., Furuya, T. and Ikura, M. (1999) *Nat. Struct. Biol.* 6, 819–824.
- [12] Elshorst, B., Hennig, M., Försterling, H., Diener, A., Maurer, M., Schulte, P., Schwalbe, H., Griesinger, C., Krebs, J., Schmid, H., Vorherr, T. and Carafoli, E. (1999) *Biochemistry* 38, 12320–12332.
- [13] Schumacher, M.A., Rivard, A.F., Bächinger, H.P. and Adelman, J.P. (2001) *Nature* 410, 1120–1124.
- [14] Drum, C.L., Yan, S.-Z., Bard, J., Shen, Y.-Q., Lu, D., Soelaiman, S., Grabarek, Z., Bohm, A. and Tang, W.-J. (2002) *Nature* 415, 396–402.
- [15] Han, B.-G., Nunomura, W., Takakuwa, Y., Mohandas, N. and Jap, B.K. (2000) *Nat. Struct. Biol.* 7, 871–875.
- [16] Yaswen, P., Smoll, A., Peehl, D.M., Trask, D.K., Sager, R. and Stampfer, M.R. (1990) *Proc. Natl. Acad. Sci. USA* 87, 7360–7364.
- [17] Rhyner, J.A., Koller, M., Durussel-Gerber, I., Cox, J.A. and Strehler, E.E. (1992) *Biochemistry* 31, 12826–12832.
- [18] Yaswen, P., Smoll, A., Hosoda, J., Parry, G. and Stampfer, M.R. (1992) *Cell Growth Differ.* 3, 335–345.
- [19] Rogers, M.S., Foley, M.A., Crotty, T.B., Hartmann, L.C., Ingle, J.N., Roche, P.C. and Strehler, E.E. (1999) *Neoplasia* 1, 220–225.
- [20] Edman, C.F., George, S.E., Means, A.R., Schulman, H. and Yaswen, P. (1994) *Eur. J. Biochem.* 226, 725–730.
- [21] Harris, E., Yaswen, P. and Thorner, J. (1995) *Mol. Gen. Genet.* 247, 137–147.
- [22] Hendrickson, W.A., Horton, J.R. and LeMaster, D.M. (1990) *EMBO J.* 9, 1665–1672.
- [23] Otwinoski, Z. and Minor, W. (1997) *Methods Enzymol.* 276, 307–326.
- [24] Terwilliger, T.C. (1994) *Acta Crystallogr. D* 50, 17–23.
- [25] Collaborative Computational Project, Number 4 (1994) *Acta Crystallogr. D* 50, 760–763.
- [26] Jones, T.A., Zou, J.-Y., Cowan, S.W. and Kjeldgaard, M. (1991) *Acta Crystallogr. A* 47, 110–119.
- [27] Brünger, A.T., Adams, P.D., Clore, G.M., DeLano, W.L., Gros, P., Grosse-Kunstleve, R.W., Jiang, J.-S., Kuszewski, J., Nilges, M., Pannu, N.S., Read, R.J., Rice, L.M., Simonson, T. and Warren, G.L. (1998) *Acta Crystallogr. D* 54, 905–921.
- [28] Kraulis, P.J. (1991) *J. Appl. Crystallogr.* 24, 946–950.
- [29] Merritt, E.A. and Murphy, M.E.P. (1994) *Acta Crystallogr. D* 50, 869–873.
- [30] Barbato, G., Ikura, M., Kay, L.E., Pastor, R.W. and Bax, A. (1992) *Biochemistry* 31, 5269–5278.
- [31] Tokumitsu, H., Wayman, G.A., Muramatsu, M. and Soderling, T.R. (1997) *Biochemistry* 36, 12823–12827.
- [32] Wayman, G.A., Tokumitsu, H. and Soderling, T.R. (1997) *J. Biol. Chem.* 272, 16073–16076.
- [33] Pearlman, D.A., Case, D.A., Caldwell, J.W., Ross, W.S., Cheatham, T.E., DeBolt, S., Ferguson, D., Seibel, G. and Kollman, P. (1995) *Comp. Phys. Commun.* 91, 1–41.